

Electronic inhomogeneity in *n*- and *p*-type PbTe detected by ^{125}Te NMRE. M. Levin,^{1,2,*} J. P. Heremans,^{3,4} M. G. Kanatzidis,^{5,6} and K. Schmidt-Rohr^{1,7}¹*Division of Materials Sciences and Engineering, Ames Laboratory US Department of Energy (DOE), Ames, Iowa 50011, USA*²*Department of Physics and Astronomy, Iowa State University, Ames, Iowa 50011, USA*³*Department of Physics, Ohio State University, Columbus, Ohio 43210, USA*⁴*Department of Mechanical and Aerospace Engineering, Ohio State University, Columbus, Ohio 43210, USA*⁵*Department of Chemistry, Northwestern University, Evanston, Illinois 60208, USA*⁶*Division of Materials Sciences, Argonne National Laboratory US DOE, Argonne, Illinois 60439, USA*⁷*Department of Chemistry, Iowa State University, Ames, Iowa 50011, USA*

(Received 16 July 2013; published 30 September 2013)

^{125}Te nuclear magnetic resonance spectra and spin-lattice relaxation of *n*- and *p*-type PbTe, self-doping narrow band-gap semiconductors, have been studied and compared to those of *p*-type GeTe. Spin-lattice relaxation in GeTe can be fit by one component, while that in both PbTe samples must be fit by at least two components, showing electronically homogeneous and inhomogeneous materials, respectively. For PbTe-based materials, the spin-lattice relaxation rate $1/T_1$ increases linearly with carrier concentration. The data for GeTe fall on the same line and allow us to extend this plot to higher concentrations. Long and short T_1 components in both PbTe samples reflect “low,” $\sim 10^{17} \text{ cm}^{-3}$, and “high,” $\sim 10^{18} \text{ cm}^{-3}$, carrier concentration components. Carrier concentrations in both *n*- and *p*-type PbTe samples obtained from the Hall and Seebeck effects generally match the “high” carrier concentration component, and to some extent, ignore the “low” one. This demonstrates that the Hall and Seebeck effects may have a limited ability for the determination of carrier concentration in complex thermoelectric PbTe-based and other multicomponent materials.

DOI: [10.1103/PhysRevB.88.115211](https://doi.org/10.1103/PhysRevB.88.115211)

PACS number(s): 72.80.Ey, 76.60.-k

I. INTRODUCTION

PbTe is a well-known self-doping narrowband gap semiconductor, which has been used for a long time and continues to attract attention as a promising matrix for thermoelectric materials.^{1–4} Depending on the Pb:Te ratio, Te or Pb vacancies may occur in PbTe, generating mobile (free) electrons or holes and resulting in *n*- or *p*-type electrical conductivity, respectively.⁵ In addition, electrons or holes in PbTe-based materials can be generated by various dopants.^{2–4,6,7} For a better understanding of thermoelectric phenomena in complex tellurides, it is necessary to control the carrier concentration, which strongly affects the Seebeck coefficient (thermopower), as well as electrical and thermal conductivities. The carrier concentration in metals and semiconductors can be derived from Hall effect measurements; in addition, the carrier concentration in PbTe-based materials can be obtained from the value of the Seebeck coefficient at 300 K via the Pisarenko relation.⁸ It is important to be sure that both methods provide the carrier concentration in thermoelectric materials correctly.

However, the Hall and Seebeck effects show *integral* properties, and the presence of even small amounts of a second phase can affect measured parameters.^{9–12} In addition, spatial electronic inhomogeneity, i.e., nonuniform carrier concentration, can be observed in materials containing two and more elements.¹³ Electronic inhomogeneity has been proposed to affect the density of electron states and superconductivity in the heavy fermion system $\text{Bi}_2\text{Sr}_2\text{CaCu}_2\text{O}_{8+x}$ ¹⁴ and the properties of the Mn-doped Ge ferromagnetic semiconductor.¹⁵ It can even result in the simultaneous presence of *n*- and *p*-type phases, which was observed by a scanning Seebeck microprobe for PbTe doped with Ag and Sb.¹⁶

^{125}Te nuclear magnetic resonance (NMR) is a powerful tool for studying *microscopic* properties of tellurides, including the

local carrier concentration.¹⁷ Mobile electrons in metals and semiconductors provide nuclear relaxation via hyperfine Fermi contact interaction with nuclear spins.¹⁸ Correlating the ^{125}Te NMR spin-lattice relaxation time T_1 and carrier concentration for electronically homogeneous PbTe-based materials, we have shown¹⁷ that T_1 can be used for the determination of the carrier concentration in multicomponent thermoelectric tellurides, including electronically inhomogeneous, e.g., $\text{Pb}_{1-x}\text{Sb}_x\text{Te}$, $\text{PbSb}_x\text{Te}_{1-x}$,⁷ and $\text{Ag}_{0.53}\text{Sb}_{1.2}\text{Pb}_{18}\text{Te}_{20}$ ¹⁷ alloys. Note also that electronic inhomogeneity recently was observed in PbTe by Taylor *et al.*¹⁹ using ^{125}Te NMR. Here, we show that measurements of the ^{125}Te NMR spin-lattice relaxation time allow us to detect electronic inhomogeneity in both *n*- and *p*-type PbTe samples, while another binary telluride, *p*-type GeTe, can be considered as electronically homogeneous. We have also expanded the plot converting T_1 to the carrier concentration reported earlier in Ref. 17, determined the local carrier concentrations in PbTe-based materials from T_1 measurements, and compared these values with those obtained from the Hall and Seebeck effects measurements.

II. EXPERIMENTAL DETAILS

Two PbTe samples, one *n*-type with Pb excess (Te vacancies), synthesized at Northwestern University (NU), and one *p*-type with Te excess (Pb vacancies), synthesized at Ohio State University (OSU), as well as *n*-type $\text{Ag}_{0.86}\text{SbPb}_{18}\text{Te}_{20}$ ¹⁷ (NWU) and *p*-type $\text{Pb}_{49.75}\text{Na}_{0.25}\text{Te}_{50}$ (OSU) samples were used in our study (see details for synthesis of tellurides in Refs. 2–4 and 8). In addition, *n*-type $\text{Pb}_{50}\text{Te}_{49.92}\text{I}_{0.08}$ and *p*-type GeTe and $\text{Ge}_{46}\text{Bi}_4\text{Te}_{50}$ samples were synthesized in the Materials Preparation Center at Ames Laboratory US Department of Energy. XRD patterns were obtained on powder

samples using a Scintag SDS-2000 diffractometer with $\text{Cu-}K_\alpha$ radiation ($\lambda = 0.154$ nm); all samples studied are single-phase materials. ^{125}Te NMR experiments were performed at 126 MHz on a Bruker Biospin (Billerica, MA) DSX-400 spectrometer in a magnetic field of 9.39 T. ^{125}Te spin-lattice relaxation was measured using saturation recovery mostly without sample spinning (static regime). In a few materials, including GeTe, $\text{Pb}_{50}\text{Te}_{49.92}\text{I}_{0.08}$, and $\text{Ag}_{0.86}\text{SbPb}_{18}\text{Te}_{20}$ it was measured with 22-kHz magic-angle spinning (MAS) in 2.5-mm rotors, which improves spectral resolution in PbTe alloys¹⁷ and averages a potential orientation dependence of T_1 . Shifts in resonance frequency due to rotation-induced sample heating were measured to be small: <20 ppm.

The uncertainty of spin-lattice relaxation time measurements in our ^{125}Te NMR experiment varies between 4 and 20%, depending on the material studied. The spin-lattice relaxation times, T_1 , were determined by fitting dependence of normalized integral vs saturation recovery time using the equations $I = 1 - e^{-t/T_1}$ or $I = f_A(1 - e^{-t/T_{1,A}}) + f_B(1 - e^{-t/T_{1,B}})$. More experimental details can be found in Ref. 17.

III. RESULTS AND DISCUSSION

^{125}Te NMR spectra of *n*- and *p*-type PbTe show resonances at -1880 and -1900 ppm, respectively [Figs. 1(a) and 1(b)], from dissolved $\text{Te}(\text{OH})_6$ at 0 ppm; for comparison, the spectrum of *p*-type GeTe with a resonance at $+160$ ppm is also shown [Fig. 1(c)]. Note that chemical shifts relative to $(\text{CH}_3)_2\text{Te}$ in benzene are higher by $+712$ ppm. There is overwhelming evidence that GeTe contains a large number of Ge vacancies with very low formation energy; these vacancies generate holes and result in *p*-type conductivity.¹⁹ As a result, the carrier concentration in GeTe is at least one order of magnitude higher than that observed in PbTe,¹⁷ and their large difference in resonance frequency can be attributed in part to a large Knight shift in GeTe, which agrees well with the short T_1 observed in GeTe (see below). In a NMR study of PbTe-GeTe alloys, we have estimated the chemical shift of GeTe to be approximately -900 ppm from $\text{Te}(\text{OH})_6$ at 0 ppm.²⁰

Figure 2 shows the normalized integral I of the ^{125}Te NMR signal for *n*-type [Fig. 2(a)] and *p*-type [Fig. 2(b)] PbTe vs saturation recovery time reflecting spin-lattice relaxation of Te nuclear spins. The insets in Figs. 2(a) and 2(b) show $(1-I)$ vs saturation recovery time and demonstrate that the ^{125}Te NMR relaxation in both PbTe samples can be fit by two components similarly as in $\text{Ag}_{0.56}\text{Sb}_{1.2}\text{Pb}_{18}\text{Te}_{20}$.¹⁷ The first component A with shorter spin-lattice relaxation time $T_{1,A}$ has a fraction f_A , and the second B with longer $T_{1,B}$ has a fraction f_B . For *n*-type PbTe, $f_A = 0.35$ and $f_B = 0.65$, and the spin-lattice relaxation times are $T_{1,A} = 2$ s and $T_{1,B} = 23$ s. For *p*-type PbTe, $f_A \approx f_B \approx 0.5$, and $T_{1,A} = 0.6$ s and $T_{1,B} = 6.0$ s. A similar biexponential spin-lattice relaxation was reported in Ref. 21 for *p*-type PbTe. In contrast to undoped *p*- and *n*-types PbTe, spin-lattice relaxation in *p*-type $\text{Pb}_{49.75}\text{Na}_{0.25}\text{Te}_{50}$ and in *n*-type $\text{Pb}_{50}\text{Te}_{49.92}\text{I}_{0.08}$ can be fit quite well by one component of $T_1 = 0.15$ s [see Fig. 3(a)] and $T_1 = 0.11$ s (not shown here), respectively. Hence, doping of PbTe with sodium or iodine is, in general, favorable for electronic homogeneity of the material. Single-component ^{125}Te NMR spin-lattice relaxation is also found for GeTe [Fig. 3(b)], i.e., GeTe is electronically

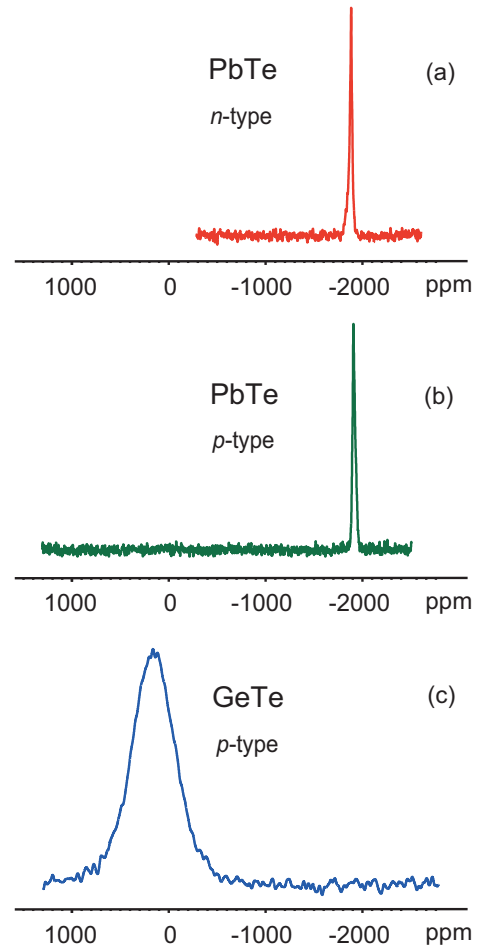


FIG. 1. (Color online) ^{125}Te NMR spectra of (a) *n*-type PbTe, (b) *p*-type PbTe, and (c) *p*-type GeTe. The scale (parts per million) is referenced to $\text{Te}(\text{OH})_6$ in solution, with TeO_2 at $+750$ ppm as a secondary reference;¹⁷ chemical shifts relative to $(\text{CH}_3)_2\text{Te}$ in benzene are higher by $+712$ ppm.

homogeneous. Figure 3(b) also compares ^{125}Te NMR spin-lattice relaxation in GeTe without spinning and at 22-kHz MAS; no significant difference is seen. Spin-lattice relaxation with and without sample spinning for the $\text{Pb}_{50}\text{Te}_{49.92}\text{I}_{0.08}$ sample has also been found to be similar. Hence, both methods reflect spin-lattice relaxation similarly, and either can be used for the determination of T_1 in PbTe- and GeTe-based materials.

Figure 4 shows the relation between the ^{125}Te NMR spin-lattice relaxation time T_1 and carrier concentration in a log-log plot. Note that a log-log plot is more convenient than a direct (linear-linear) plot because the data are distinguishable not only at high, but also at low carrier concentrations, and it allows us to convert spin-lattice relaxation time to carrier concentration over a wide range of values. Similar dependencies based on ^{125}Te as well as on ^{207}Pb NMR were reported by us earlier for the *n*-type PbTe-based materials only.¹⁷ For the plot shown in Fig. 4, we used *n*- and *p*-type PbTe-based materials: *n*-type $\text{Ag}_{0.86}\text{SbPb}_{18}\text{Te}_{20}$ and $\text{Pb}_{50}\text{Te}_{49.92}\text{I}_{0.08}$ and *p*-type $\text{Pb}_{49.75}\text{Na}_{0.25}\text{Te}_{50}$. Spin relaxation in all these samples can be fit by one component, and they can be considered as electronically homogeneous: an example of one-component ^{125}Te NMR spin-lattice relaxation

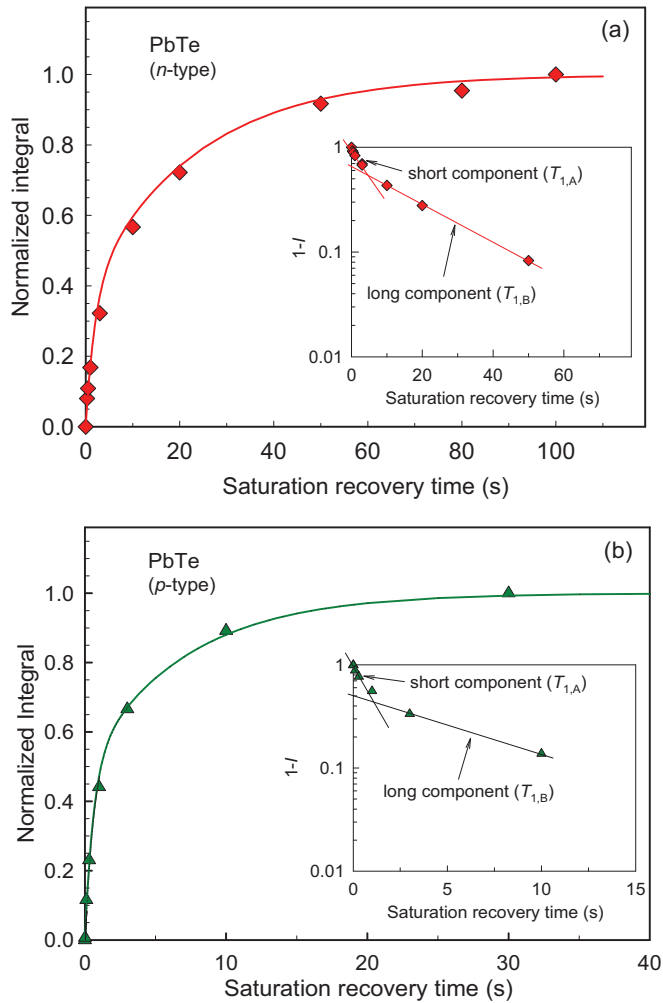


FIG. 2. (Color online) Normalized integral I of ^{125}Te NMR signal vs saturation recovery time for (a) *n*- and (b) *p*-type PbTe samples. Insets in (a) and (b) show semilogarithmic plots of $(1-I)$ vs saturation recovery time, which can be fit by two spin-lattice relaxation times $T_{1,A}$ and $T_{1,B}$ for two components, *A* and *B*, with fractions f_A and f_B in each sample.

is shown for $\text{Pb}_{49.75}\text{Na}_{0.25}\text{Te}_{50}$ in Fig. 3(a). In addition, we used the data for *p*-type GeTe with $T_1 = 5.3 \pm 0.2$ ms and hole concentration $p = 8 \times 10^{20} \text{ cm}^{-3}$ obtained from Hall effect measurements,²² and for *p*-type $\text{Ge}_{46}\text{Bi}_4\text{Te}_{50}$ with $T_1 = 10$ ms and $p = 2.5 \times 10^{20} \text{ cm}^{-3}$ obtained by us from Seebeck coefficient measurements and consistent with Hall-effect measurements on similar materials.²³ The experimental dependence of ^{125}Te NMR spin-lattice relaxation time vs carrier concentration for all samples studied can be fit by a straight line of slope one in the log-log plot (i.e., a linear relation between $1/T_1$ and carrier concentration), similar to that reported by us in Ref. 17, but the dependence is now expanded up to carrier concentrations of $\sim 10^{21} \text{ cm}^{-3}$. Selbach *et al.*¹⁸ showed that the NMR spin-lattice relaxation time T_1 in semiconductors depends on the concentration of mobile charge carriers n , as follows

$$1/T_1 = C_B n T^{1/2}, \quad (1)$$

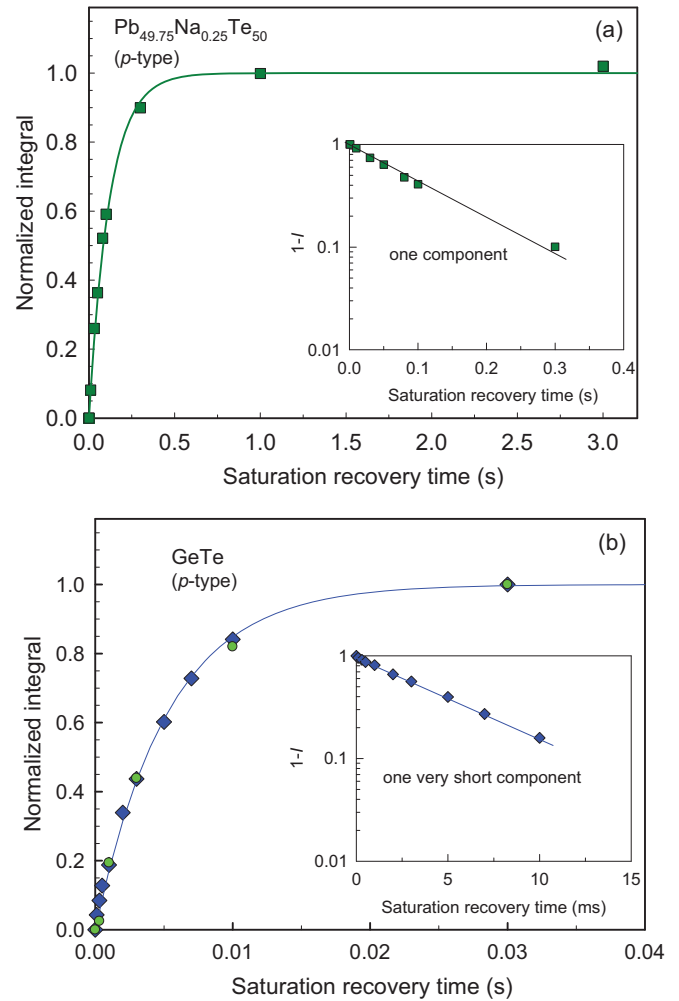


FIG. 3. (Color online) Normalized integral I of the ^{125}Te NMR static signal vs saturation recovery time for *p*-type (a) $\text{Pb}_{49.75}\text{Na}_{0.25}\text{Te}_{50}$ and (b) GeTe. Green circles in (b) show ^{125}Te MAS 22-kHz NMR data for the same GeTe sample in the same 2.5-mm rotor. Insets show semilogarithmic plots of $(1-I)$ vs saturation recovery time, which can be fit by one T_1 component for both samples.

where C_B is the Bloembergen constant and T is the absolute temperature. Equation (1) shows that for similar materials, at the same temperature, the spin-lattice relaxation rate $1/T_1$ is proportional to the carrier concentration. Our data of spin-lattice relaxation time vs charge carrier concentration in Fig. 4 agree with this theoretical prediction (straight line), which can be used to obtain the carrier concentration over a wide range of T_1 values in complex tellurides.

It should be noted here that nuclear spin relaxation in semiconductors observed by NMR can be affected not only by charge carriers but also by phonons.^{18,24} However, the effect of phonons on nuclear spin relaxation at 300 K in pure tellurium has been shown to be much weaker than that due to conduction electrons.^{18,24} Our data also show that if 4 at.% Ge in GeTe is replaced by Bi, T_1 increases while carrier concentration decreases (see above), and the point for $\text{Ge}_{46}\text{Bi}_4\text{Te}_{50}$ falls on the line of $1/T_1$ vs carrier concentration (Fig. 4). Hence, very short T_1 observed for GeTe can be attributed mostly to high carrier concentration, which is much higher than in both PbTe

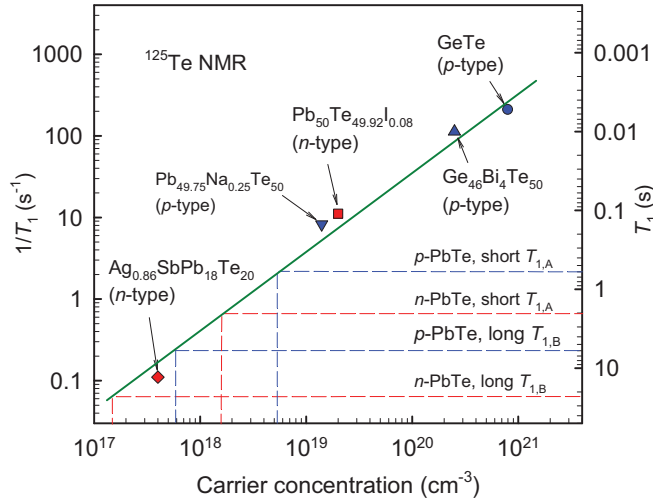


FIG. 4. (Color online) ^{125}Te NMR spin-lattice relaxation rate $1/T_1$ vs carrier concentration in n - and p -type tellurides. The relation was plotted on the basis of ^{125}Te NMR spin-lattice relaxation times and carrier concentrations obtained from Hall and Seebeck effects for n -type $\text{Ag}_{0.86}\text{SbPb}_{48}\text{Te}_{20}$ and $\text{Pb}_{50}\text{Te}_{49.92}\text{I}_{0.08}$ and p -type $\text{Pb}_{49.75}\text{Na}_{0.25}\text{Te}_{50}$, $\text{Ge}_{46}\text{Bi}_4\text{Te}_{50}$, and GeTe ; all these samples exhibit nearly single-exponential T_1 relaxation. A straight line of slope 1.0, i.e., the linear relation between $1/T_1$ and carrier concentration expected from theory, is also shown in the plot. ^{125}Te NMR short, $T_{1,A}$, and long, $T_{1,B}$, relaxation components were determined for n - and p -type PbTe samples (horizontal dashed lines) and converted to carrier concentrations (vertical dashed lines), demonstrating to what extent both PbTe samples are electronically inhomogeneous.

samples, and agrees well with the Knight shift being much larger than for both n - and p -type PbTe samples (Fig. 1).

Our data in Fig. 4 show that a particularly attractive feature of ^{125}Te NMR is the possibility to obtain the carrier concentration in complex tellurides in the range of $\sim 10^{17}$ to 10^{21} cm^{-3} with single- or biexponential spin-lattice relaxation, i.e., in electronically homogeneous or inhomogeneous materials, respectively. Using this plot, we have converted T_1 measured for n - and p -types PbTe (horizontal dashed lines in Fig. 4) to carrier concentration (vertical dashed lines in Fig. 4) and compared the obtained carrier concentration values with those measured in the same samples by the Hall or Seebeck effects. The two ^{125}Te NMR spin-lattice relaxation times measured for n - and p -type PbTe samples can be associated with regions with different carrier concentrations: in the n -type PbTe sample, “high” $n = 1.5 \times 10^{18}$ cm^{-3} and “low” $n = 1.5 \times 10^{17}$ cm^{-3} and in the p -type PbTe sample, “high” $p = 5 \times 10^{18}$ cm^{-3} and “low” $p = 5 \times 10^{17}$ cm^{-3} . The carrier concentrations within these PbTe samples are different by about one order of magnitude, similar to PbTe doped with Ag and Sb (lead-antimony-silver-tellurium, LAST- m materials).¹⁷ Depending on the Pb:Te ratio and parameters of synthesis, PbTe samples certainly may have different “low” and “high” carrier concentrations.

One of the problems with electronically inhomogeneous systems is a determination of the contributions from different phases to the Hall and Seebeck effects.^{10,13} The Seebeck coefficient and power factor of systems containing two phases with high and low thermopower has been studied theoretically¹¹ and

experimentally;¹² the resulting thermopower depends on the magnitude and sign of the thermopower of these phases and on the fractions of these phases. Wolfe *et al.*⁹ have shown that at 300 K, the Hall coefficient of AgSbTe_2 is positive in some specimens and negative in others, while the Seebeck coefficient is always positive; it was suggested that different types of conductivity can be attributed to different phases, AgSbTe_2 and Ag_2Te , occurring in the ingot during solidification. Hence, the presence of phases with different type and/or concentration of charge carriers, i.e., electronic inhomogeneity, interfere with a quantitative evaluation of the data obtained from Hall and Seebeck effects.

Thus, it is difficult, if not impossible, to determine the electronic inhomogeneity in tellurides using common Seebeck or Hall effect measurements, while ^{125}Te NMR can achieve this. The carrier concentrations determined in n -type and p -type PbTe samples from the Seebeck or Hall effects are $n = 1.2 \times 10^{18}$ cm^{-3} and $p = 4.0 \times 10^{18}$ cm^{-3} , respectively. Hence, carrier concentrations obtained from the Seebeck and Hall effects measurements generally match the “high” carrier concentration in both n - and p -type PbTe samples, associated with the short ^{125}Te NMR T_1 component. Because intrinsic carriers in PbTe can be generated in sufficient concentrations only at temperatures above ~ 700 K, the variation in carrier concentration in n - and p -type PbTe at 300 K can be attributed to a spatial variation of Pb and Te vacancy concentration. A discrepancy between the measured and real carrier concentration can, in principle, be the reason for reported deviations from the Pisarenko relation between the Seebeck coefficient and carrier concentration in PbTe-based materials.⁸

The position of the NMR resonance is determined by the chemical environment (chemical shift) and carrier concentration (Knight shift), whereas its width is determined by a distribution of chemical and Knight shifts. The much wider ^{125}Te NMR signal for GeTe compared to that of PbTe can be attributed to a wider distribution of Knight shifts due to the large absolute value: for an average Knight shifts of 1000 ppm, a $\pm 20\%$ distribution in the carrier concentration results in a 400-ppm line broadening. Strictly speaking, GeTe may also be electronically inhomogeneous but to a much smaller extent than PbTe.

IV. CONCLUSIONS

^{125}Te NMR data show that both n - and p -types PbTe samples are electronically inhomogeneous, while GeTe is mostly homogeneous. This can be explained by a spatial variation of the Pb:Te ratio, i.e., concentration of Pb or Te vacancies generating holes and/or electrons, respectively, resulting in different local spin-lattice relaxation. Doping of PbTe with sodium or iodine results in better homogeneity of the carrier concentration. While ^{125}Te NMR detects both the “high” and “low” carrier concentration, the Hall or Seebeck effects reflect mostly “high” carrier concentration, which can be misleading in some PbTe-based and other multicomponent materials.

ACKNOWLEDGMENTS

The authors thank C. M. Jaworski (OSU), K. Ahn (NU), and the Materials Preparation Center at Ames Laboratory US

DOE for sample synthesis. The NMR study was supported by the US DOE of Basic Energy Sciences (BES), Division of Materials Sciences and Engineering, and performed at the Ames Laboratory, which is operated for the US DOE by Iowa State University under Contract No. DE-AC02-07CH11358.

Work at OSU was supported by NSF-CBET, Award No. 1048622. Work at NU was supported by the Energy Frontier Research Center Revolutionary Materials for Solid State Energy Conversion, funded by US DOE, BES, under Award No. DE-SC0001054.

*Corresponding author: levin@iastate.edu

- ¹G. J. Snyder and E. S. Toberer, *Nat. Mater.* **7**, 105 (2008).
- ²Y. Pei, X. Shi, A. LaLonde, H. Wang, L. Chen, and G. J. Snyder, *Nature (London)* **473**, 66 (2011).
- ³J. P. Heremans, V. Jovovic, E. S. Toberer, A. Saramat, K. Kurosaki, A. Charoenphakdee, S. Yamanaka, and G. J. Snyder, *Science* **321**, 554 (2008).
- ⁴K. Biswas, J. He, I. D. Blum, C. I. Wu, T. P. Hogan, D. N. Seidman, V. P. Dravid, and M. G. Kanatzidis, *Nature (London)* **489**, 414 (2012).
- ⁵N. J. Parada and G. W. Pratt, Jr., *Phys. Rev. Lett.* **22**, 180 (1969).
- ⁶S. Ahmad, S. D. Mahanti, K. Hoang, and M. G. Kanatzidis, *Phys. Rev. B* **74**, 155205 (2006).
- ⁷C. M. Jaworski, J. Tobola, E. M. Levin, K. Schmidt-Rohr, and J. P. Heremans, *Phys. Rev. B* **80**, 125208 (2009).
- ⁸J. P. Heremans, C. M. Thrush, and D. T. Morelli, *J. Appl. Phys.* **98**, 063703 (2005).
- ⁹R. Wolfe, J. H. Wernick, and E. Haszko, *J. Appl. Phys.* **31**, 1959 (1960).
- ¹⁰C. Herring, *J. Appl. Phys.* **31**, 1939 (1960).
- ¹¹D. J. Bergman and L. G. Fel, *J. Appl. Phys.* **85**, 8205 (1999).
- ¹²J. P. Heremans and C. M. Jaworski, *Appl. Phys. Lett.* **93**, 122107 (2008).
- ¹³A. Y. Shik, *Electronic Properties of Inhomogeneous Semiconductors* (Gordon and Breach Publishers, Australia, US, 1995).
- ¹⁴S. H. Pan, J. P. O'Neal, R. L. Badzey, C. Chamon, H. Ding, J. R. Engelbrecht, Z. Wang, H. Eisaki, S. Uchida, A. K. Gupta, K. W. Ng, E. W. Hudson, K. M. Lang, and J. C. Davis, *Nature (London)* **413**, 282 (2001).
- ¹⁵J. S. Kang, G. Kim, S. C. Wi, S. S. Lee, S. Choi, S. Cho, S. W. Han, K. H. Kim, H. J. Song, H. J. Shin, A. Sekiyama, S. Kasai, S. Suga, and B. I. Min, *Phys. Rev. Lett.* **94**, 147202 (2005).
- ¹⁶N. Chen, F. Gascoin, G. J. Snyder, E. Muller, G. Karpinski, and C. Stiewe, *Appl. Phys. Lett.* **87**, 171903 (2005).
- ¹⁷E. M. Levin, B. A. Cook, K. Ahn, M. G. Kanatzidis, and K. Schmidt-Rohr, *Phys. Rev. B* **80**, 115211 (2009).
- ¹⁸H. Selbach, O. Kanert, and D. Wolf, *Phys. Rev. B* **19**, 4435 (1979).
- ¹⁹A. H. Edwards, A. C. Pineda, P. A. Schultz, M. G. Martin, A. P. Thompson, H. P. Hjarson, and C. J. Umrigar, *Phys. Rev. B* **73**, 045210 (2006).
- ²⁰B. Njegic, E. M. Levin, and K. Schmidt-Rohr [Solid State Nucl. Magn. Reson. (2013)] (to be published).
- ²¹R. E. Taylor, F. Alkan, D. Koumoulis, M. P. Lake, D. Kong, C. Dybowski, and L. S. Bouchard, *J. Phys. Chem. C* **117**, 8959 (2013).
- ²²E. M. Levin, M. F. Besser, and R. Hanus, *J. Appl. Phys.* **114**, 083713 (2013).
- ²³M. S. Lubell and Mazelsky, *J. Electrochem. Soc.* **110**, 520 (1963).
- ²⁴A. Koma, A. Hojo, and S. Tanaka, *Phys. Lett. A* **28**, 95 (1968).